Highly reddened Type Ia supernova SN 2004ab: another case of anomalous extinction

N. K. Chakradhari,[1]⋆† D. K. Sahu,[2]† G. C. Anupama[2] and T. P. Prabhu[2]

[1]*School of Studies in Physics & Astrophysics, Pt. Ravishankar Shukla University, Raipur 492010, India*
[2]*Indian Institute of Astrophysics, Koramangala, Bangalore 560 034, India*

ABSTRACT

We present optical photometric and spectroscopic data for supernova SN 2004ab, a highly reddened normal Type Ia supernova. The total reddening is estimated as $E(B - V) = 1.70 \pm 0.05$ mag. The intrinsic decline-rate parameter $\Delta m_{15}(B)_{\text{true}}$ is 1.27 ± 0.05, and the B-band absolute magnitude at maximum $M_B^{\max}$ is -19.31 ± 0.25 mag. The host galaxy NGC 5054 is found to exhibit anomalous extinction with a very low value of $R_V = 1.41 \pm 0.06$ in the direction of SN 2004ab. The peak bolometric luminosity is derived as $\log L_{\text{bol}}^{\max} = 43.10 \pm 0.07$ erg s^{-1}. The photospheric velocity measured from the absorption minimum of the Si II λ6355 line shows a velocity gradient of $\dot{v} = 90$ km s^{-1} d^{-1}, indicating that SN 2004ab is a member of the high velocity gradient (HVG) subgroup. The ratio of the strengths of the Si II λ5972 and λ6355 absorption lines, $\mathcal{R}(\text{Si II})$, is estimated as 0.37, while their pseudo-equivalent widths suggest that SN 2004ab belongs to the broad line (BL) type subgroup.

Key words: techniques: photometric – techniques: spectroscopic – supernovae: general – supernovae: individual: SN 2004ab – galaxies: individual: NGC 5054.

1 INTRODUCTION

The correlation of the absolute magnitude of Type Ia supernovae (SNe Ia) with their observed properties, such as the decline in the B-band magnitude from its peak to 15 d after peak (Phillips 1993; Phillips et al. 1999), the stretch parameter (Perlmutter et al. 1997), the shape of the light curve (Riess, Press & Kirshner 1996), the colour (Reindl et al. 2005; Wang et al. 2006) and the spectroscopic parameters (Nugent et al. 1995; Benetti et al. 2005), has made SNe Ia very important astronomical events, as they provide a means to calibrate the luminosity at maximum. Furthermore, the high luminosities of SNe Ia enable us to see them at great distances in the Universe and to use them as standard candles for distance estimation.

Their observed properties and theoretical investigations suggest that SNe Ia are a result of the explosion of a carbon–oxygen white dwarf (WD, Hoyle & Fowler 1960) that gains mass through accretion in a binary system or from merging with another WD. The binary companion may be a main sequence/red giant star (single-degenerate scenario; Whelan & Iben 1973) or another WD (double-degenerate scenario; Iben & Tutukov 1984; Webbink 1984). As the mass of the WD reaches the Chandrasekhar limit

(Chandrasekhar 1931), an instability sets in, leading to a thermonuclear runaway fusion reaction that disrupts the WD. However, the exact nature of the progenitor and explosion scenario are still debated (Maoz, Mannucci & Nelemans 2014) and need to be addressed properly in order for SNe Ia to be used in precision cosmology (Howell 2011).

An estimate of the reddening suffered by SNe Ia and its correction are very important when these objects are being used as distance indicators. Although the majority of SN host galaxies show extinction properties similar to that of the Milky Way, consistent with a total to selective extinction ratio of $R_V = 3.1$, this value is found to be significantly lower in the direction of SNe Ia in many host galaxies (Krisciunas et al. 2006; Elias-Rosa et al. 2006; Krisciunas et al. 2007; Wang et al. 2008; Folatelli et al. 2010; Amanullah et al. 2014). The departure of R_V from the Galactic value is generally referred to as non-standard extinction. Several studies suggest that non-standard extinction with R_V lower than 3.1 is shown mostly by SNe Ia that are significantly reddened (Jha, Riess & Kirshner 2007; Folatelli et al. 2010; Chotard et al. 2011; Mandel, Narayan & Kirshner 2011; Scolnic et al. 2014).

The reddening of SNe Ia arises from at least two sources: the first one, causing a small amount of reddening and seen in most SNe Ia, is consistent with the properties of interstellar dust in the Milky Way, while the second, responsible for reddening in the high-extinction objects, is characterized by an unusually low value of R_V (Phillips 2012). Wang (2005) and Goobar (2008) suggest that the low value of R_V could result from multiple scatterings of light

⋆ Centre for Mega Projects in Multiwavelength Astronomy, Pt. Ravishankar Shukla University Raipur.
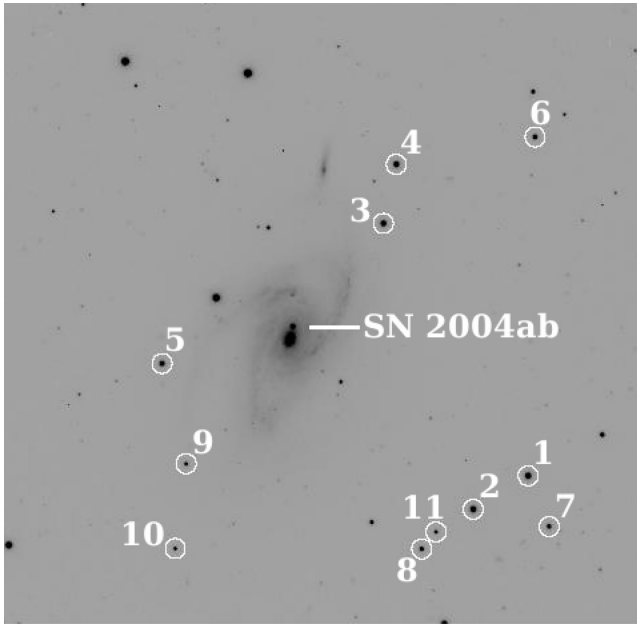† E-mail: nkchakradhari@gmail.com (NKC); dks@iiap.res.in (DKS)

Figure 1. Identification chart for SN 2004ab. The stars used as local secondary standards are marked as numbers 1–11, and their calibrated magnitudes are listed in Table 1. North is up and east is to the left. The field of view is 10×10 arcmin^2.

owing to the dust in the circumstellar medium (CSM). Goobar (2008) and Amanullah et al. (2014) have shown that the extinction properties of highly reddened objects with low values of R_V follow a power law.

In this paper, we present optical *BVRI* photometric and medium-resolution spectroscopic analyses of the highly reddened Type Ia supernova SN 2004ab. It was discovered on 2004 February 21.98 (UT), at 2 arcsec west and 11 arcsec north (see Fig. 1) of the centre of NGC 5054 (Monard & Vanmunster 2004). NGC 5054 is an SA(s)bc type galaxy at a redshift of $z = 0.0058$ (Pisano et al. 2011, source NED). SN 2004ab was classified as a Type Ia supernova on February 24 and suggested to be a highly reddened supernova, caught about 1 week after maximum light. The expansion velocity measured using an absorption minimum of Si II λ6355 was $10\,400\,\mathrm{km\,s^{-1}}$ (Matheson et al. 2004).

The paper is organized as follows. Section 2 describes the observation and data reduction techniques. The photometric results are presented in Section 3. The anomalous extinction of the host galaxy NGC 5054 is discussed in Section 4. Absolute and bolometric luminosities are estimated in Section 5. Spectroscopic results are presented in Section 6. The paper is summarized in Section 7.

2 OBSERVATIONS AND DATA REDUCTION

2.1 Imaging

Observations of SN 2004ab were carried out using the Himalaya Faint Object Spectrograph Camera (HFOSC) attached to the 2-m Himalayan Chandra Telescope (HCT) of the Indian Astronomical Observatory (IAO), Hanle, India. HFOSC is equipped with $2K \times 4K$ pixel and a SITe CCD chip. The central $2K \times 2K$ pixels of the chip, with a field of view of 10×10 arcmin^2, at a plate scale of 0.296 arcsec pixel^{-1} were used for imaging observations. The HFOSC CCD has a gain of 1.22 electron ADU^{-1} and a readout noise of 4.87 electrons.

The photometric monitoring of SN 2004ab began on 2004 February 24 and continued until 2004 June 22 in Bessel's *B*, *V*, *R* and *I* filters. Landolt (1992) standard star fields were observed on 2004 February 24 (PG0918+029, PG0942-029, SA101, SA104), March 1 (PG0918+029, PG1047+003, PG1323-086, PG1530+057), March 10 (PG0918+029, PG0942-029, PG1047+003, PG1323-086) and May 11 (PG1633+099, PG1657+078, SA107) under photometric conditions. These fields were used to estimate the atmospheric extinction and transformation coefficients, and to calibrate a sequence of secondary standards in the supernova field. Standard fields were monitored in the airmass range ∼1.1–2.0 for estimating atmospheric extinction, whereas for determining transformation coefficients the airmass range was restricted to ∼1.1–1.4.

The CCD images were processed using standard IRAF[1] routines. The images were bias-corrected with a median-combined master bias frame obtained using all the bias frames taken throughout the night. Flat-field correction was performed using the median-combined normalized flat-field images of the twilight sky in different bands. Cosmic ray hits were removed from the flat-field-corrected images.

Aperture photometry was performed on the stars of Landolt standard fields using the IRAF DAOPHOT package. Bright stars in the Landolt standard field were used to determine the aperture growth curve and to compute aperture corrections by measuring the magnitude difference at an aperture radius ∼3–4 times the full width at half-maximum (FWHM) and at an aperture close to the FWHM of the stellar profile. The magnitudes of Landolt standard stars were obtained by applying the aperture corrections to the magnitude determined at a radius (close to the FWHM) that maximized the signal-to-noise (S/N) ratio. The nightly extinction coefficients in the various bands were determined. The observed magnitudes of the Landolt standards were corrected for atmospheric extinction using the estimated nightly extinction coefficients. Finally, the corrected magnitudes of Landolt standards were used to derive the colour terms and photometric zero-points on each night.

We selected a sequence of stars in the field of SN 2004ab (marked in Fig. 1) to use as secondary standards. Aperture photometry, as discussed above, was performed on these stars on the nights when Landolt standard stars were observed. The magnitudes of this sequence of stars were determined by applying aperture corrections computed using bright stars in the field of SN 2004ab. The observed magnitudes were extinction-corrected using the nightly extinction coefficients. The extinction-corrected magnitudes were then calibrated using colour terms, and zero-points were obtained using observations of Landolt standards.

The average *BVRI* magnitudes of the sequence of secondary standards in the field of SN 2004ab are given in Table 1. The errors associated with the magnitudes of secondary standards are the standard deviation of the magnitudes obtained on the four calibration nights. These secondary standards were used to calibrate the supernova magnitude obtained on other nights.

SN 2004ab occurred close to the nucleus of the host galaxy, in a region with a very high and highly varying background (see Fig. 1). The contamination by the galaxy background prohibits a proper estimation of the supernova magnitude. Hence, the template subtraction method was used to subtract the galaxy background. The *BVRI* template frames were prepared from multiple deep exposures

---

[1] IRAF is distributed by the National Optical Astronomy Observatories, which are operated by the Association of Universities for Research in Astronomy, Inc., under cooperative agreement with the National Science Foundation.

Table 1. Magnitudes for the sequence of secondary standard stars in the field of SN 2004ab. The stars are marked in Fig. 1

ID	B	V	R	I
1	14.773 ± 0.033	14.055 ± 0.017	13.637 ± 0.017	13.246 ± 0.005
2	15.144 ± 0.035	14.227 ± 0.016	13.667 ± 0.015	13.111 ± 0.009
3	14.875 ± 0.032	14.241 ± 0.013	13.851 ± 0.018	13.475 ± 0.010
4	15.175 ± 0.031	14.347 ± 0.013	13.867 ± 0.016	13.421 ± 0.017
5	15.343 ± 0.034	14.693 ± 0.020	14.290 ± 0.023	13.921 ± 0.024
6	16.044 ± 0.024	15.226 ± 0.010	14.753 ± 0.012	14.306 ± 0.011
7	15.954 ± 0.037	15.372 ± 0.017	15.001 ± 0.016	14.627 ± 0.004
8	17.518 ± 0.048	16.082 ± 0.013	15.119 ± 0.017	14.139 ± 0.011
9	16.916 ± 0.021	16.326 ± 0.017	15.953 ± 0.014	15.581 ± 0.024
10	17.106 ± 0.022	16.456 ± 0.015	16.047 ± 0.023	15.665 ± 0.008
11	17.640 ± 0.058	16.557 ± 0.014	15.873 ± 0.016	15.278 ± 0.003

Table 3. Log of spectroscopic observations of SN 2004ab.

Date	JD^a	$Phase^b$	Range [Å]
24/02/2004	3060.50	3.68	3500–7800
25/02/2004	3061.50	4.68	3500–7800
26/02/2004	3062.43	5.61	3500–7800
28/02/2004	3064.37	7.55	3500–7800; 5200–9250
29/02/2004	3065.35	8.53	3500–7800; 5200–9250
04/03/2004	3069.36	12.54	3500–7800; 5200–9250
08/03/2004	3073.46	16.64	3500–7800; 5200–9250
14/03/2004	3079.33	22.51	3500–7800; 5200–9250
03/04/2004	3099.33	42.51	3500–7800; 5200–9250
26/04/2004	3122.20	65.38	3500–7800; 5200–9250
05/05/2004	3131.25	74.43	3500–7800; 5200–9250

Notes. ^{a}2450000+; ^{b}in days relative to the *B*-band maximum.

of host galaxy NGC 5054, obtained with the same instrumental setup and under good seeing conditions on 2005 May 28. Template frames were subtracted from the supernova frames of the respective bands. This leaves behind only the supernova. The magnitudes of the supernova and secondary standards were extracted by aperture photometry with a smaller aperture radius (∼FWHM). The aperture correction, determined using bright stars in the supernova field, was applied to the extracted magnitudes of the supernova and secondary standards. The nightly zero-points, determined from the observed and calibrated magnitudes of secondary standards and the average of derived colour terms for four nights, were used to calibrate the supernova magnitudes. As the reddening in the direction of SN 2004ab is high (see Section 4), the effect of second-order extinction was taken into account in all the calibration processes. The derived supernova magnitudes are listed in Table 2. The final error in the supernova magnitudes was estimated by adding in quadrature the photometric error at the aperture with the maximum S/N ratio (i.e. the photometric error computed by IRAF), the error in aperture correction, and the error associated with nightly photometric zero-points.

2.2 Spectroscopy

Spectroscopic observations of SN 2004ab were carried out from 2004 February 24 to May 5 on 11 occasions. Spectra were obtained

using Gr#7 (wavelength range 3500–7800 Å) and Gr#8 (wavelength range 5200–9250 Å) of the HFOSC at a spectral resolution of ∼7 Å. The log of spectroscopic observations is given in Table 3. The spectrophotometric standard stars Feige 34, Feige 66, BD +33° 2642, HZ 44 and Wolf 1346 were observed for flux calibration. All the spectral data were processed in a standard manner using various tasks in IRAF. One-dimensional spectra were extracted using the optimal extraction method. The dispersion solutions obtained using arc lamp spectra of FeNe and FeAr were used to wavelength-calibrate the supernova spectra. Wavelength-calibrated spectra were cross-checked using bright night-sky emission lines and, wherever required, small shifts were applied. Spectrophotometric standard stars observed with a broader slit on the same night or nearby nights were used to correct for the instrumental response and atmospheric extinction using the average spectroscopic extinction curve for the site. The spectra obtained in Gr#7 (blue region) and Gr#8 (red region) were combined by scaling one of the spectra to the weighted mean of the other in the overlapping region, in order to obtain a single spectrum covering the blue to red region. We performed bandpass spectrophotometry of the spectra using the transmission curves of filters available with the HFOSC. The photometric flux obtained using the available photometry was compared with the spectroscopic flux within a given bandpass, and the scale factor was determined in each band. A cubic spline curve going through the

Table 2. Optical *BVRI* photometry of SN 2004ab with the Himalayan Chandra Telescope.

Date	JD^a	$Phase^b$	B	V	R	I
24/02/2004	3060.44	3.62	16.867 ± 0.008	15.154 ± 0.006	14.461 ± 0.011	14.100 ± 0.014
25/02/2004	3061.49	4.67	16.880 ± 0.011	15.133 ± 0.007	14.450 ± 0.012	14.100 ± 0.016
26/02/2004	3062.41	5.59	16.958 ± 0.011	15.161 ± 0.014	14.479 ± 0.011	14.122 ± 0.008
27/02/2004	3063.38	6.56	17.031 ± 0.009	15.213 ± 0.009	14.532 ± 0.006	14.166 ± 0.017
28/02/2004	3064.35	7.53	17.078 ± 0.007	15.219 ± 0.008	14.586 ± 0.004	14.210 ± 0.013
29/02/2004	3065.40	8.58	17.167 ± 0.008	15.246 ± 0.005	14.638 ± 0.005	14.235 ± 0.011
01/03/2004	3066.42	9.60	17.269 ± 0.009	15.349 ± 0.008	14.739 ± 0.010	14.330 ± 0.010
04/03/2004	3069.39	12.57	17.528 ± 0.032	15.512 ± 0.011	14.890 ± 0.013	
10/03/2004	3075.39	18.57	18.315 ± 0.043	15.906 ± 0.017	15.048 ± 0.011	14.340 ± 0.018
14/03/2004	3079.28	22.46	18.726 ± 0.026	16.079 ± 0.010	15.079 ± 0.017	14.229 ± 0.020
16/03/2004	3081.33	24.51	18.903 ± 0.033	16.189 ± 0.014	15.155 ± 0.013	14.274 ± 0.017
03/04/2004	3099.26	42.44	19.772 ± 0.066	17.157 ± 0.016	16.226 ± 0.014	15.302 ± 0.014
15/04/2004	3111.26	54.44		17.532 ± 0.009	16.629 ± 0.009	15.852 ± 0.010
24/04/2004	3120.31	63.49		17.752 ± 0.013	16.890 ± 0.017	16.195 ± 0.025
05/05/2004	3131.22	74.40		18.014 ± 0.017	17.262 ± 0.017	16.634 ± 0.025
11/05/2004	3137.23	80.41		18.147 ± 0.022	17.427 ± 0.019	16.879 ± 0.026
22/05/2004	3148.12	91.30		18.493 ± 0.021	17.905 ± 0.028	17.225 ± 0.022

Notes. ^{a}2450000+; ^{b}observed phase in days with respect to the epoch of *B*-band maximum: JD = 245 3056.82.
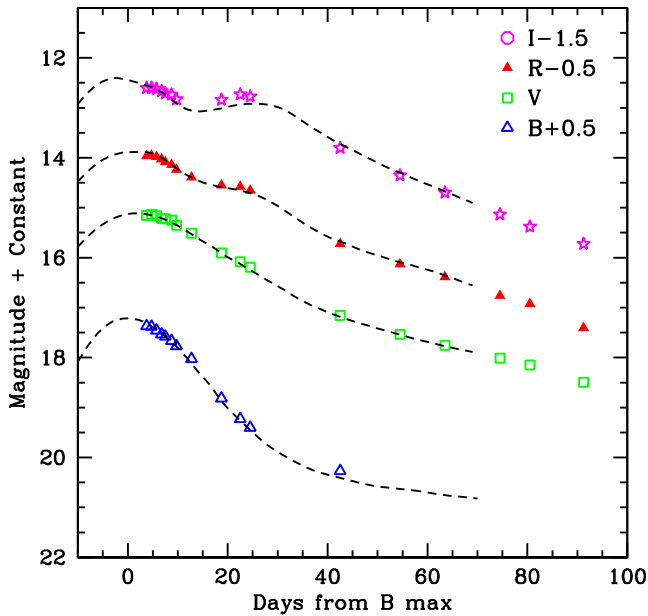
Figure 2. *BVRI* light curves of SN 2004ab. The light curves have been shifted by the amount indicated in the legend. The phase is measured in days from the *B*-band maximum. The dashed lines represent the template light curves obtained using the SNOOPY code.

scale factor in each band was fitted, and the spectra were scaled using this curve to match photometric and spectroscopic fluxes. In this way the combined spectra were brought to an absolute flux scale. The spectra were then dereddened and corrected for the redshift of the host galaxy NGC 5054, using $z = 0.0058$ (Pisano et al. 2011, source NED).

3 PHOTOMETRIC RESULTS

The *BVRI* light curves of SN 2004ab are presented in Fig. 2. SN 2004ab was discovered post-maximum, and our monitoring started $\sim$3 d after discovery. In order to determine the date of the maximum and the brightness at maximum, we used the SNOOPY (Burns et al. 2011) software package, developed by the Carnegie Supernova Project (CSP) for analysing light curves of SNe Ia.

The best-matching templates to the observed *BVRI* light curves of SN 2004ab, generated using SNOOPY, are shown in Fig. 2, along with the observed light curves. The dates of maximum and peak brightness in different bands, obtained using the template fit, are listed in Table 4. The maximum in the *V*, *R* and *I* bands occurred at $\sim$+1.5, +2.8 and -2 d, relative to the *B*-band maximum. This is in accordance with the observed trend in normal SNe Ia, where the maximum in the *I* band precedes and those in the *V* and *R* bands follow the maximum in the *B* band. The maximum brightnesses

in the *B*, *V*, *R* and *I* bands are estimated as 16.71, 15.11, 14.38 and 13.90 mag, respectively. Similar to normal SNe Ia, SN 2004ab also shows a shoulder in the *R* band and a pronounced secondary maximum in the *I* band. The secondary maximum in the *I* band is $\sim$0.5 mag fainter with respect to the first maximum and occurred after $\sim$25 d.

The decline-rate parameter, $\Delta m_{15}(B)$, for SN 2004ab is estimated as 1.17. Decline-rate parameters and the rate of light-curve decline during the late phase (40–90 d) in the *VRI* bands are estimated by a least-squares fit to the observed data and are listed in Table 4. Phillips et al. (1999) have shown that reddening acts to decrease the decline rate. Hence, the measured decline-rate parameter needs to be corrected for reddening. The observed decline-rate parameter translates to the intrinsic decline-rate parameter $\Delta m_{15}(B)_{\text{true}} = 1.27$, after correction for reddening (see Section 4), using the updated relationship derived by Folatelli et al. (2010).

In Fig. 3, the *BVRI* light curves of SN 2004ab are compared with those of SN 1996X ($\Delta m_{15}(B) = 1.31$; Salvo et al. 2001), SN 2001el ($\Delta m_{15}(B) = 1.13$; Krisciunas et al. 2003), SN 2003du ($\Delta m_{15}(B) = 1.04$; Anupama, Sahu & Jose 2005; Stanishev et al. 2007), SN 2005cf ($\Delta m_{15}(B) = 1.12$; Pastorello et al. 2007b; Wang et al. 2009b), SN 2006X ($\Delta m_{15}(B) = 1.31$; Wang et al. 2008) and SN 2011fe ($\Delta m_{15}(B) = 1.07$; Vinkó et al. 2012; Richmond & Smith 2012). All the light curves have been shifted to match their peak magnitude in the respective bands and to the epoch of the *B*-band maximum. The *B*-band light curve of SN 2004ab closely resembles those of SN 2001el, SN 2003du, SN 2005cf and SN 2011fe (until $\sim$25 d). In the *V* and *R* bands, the light curve of SN 2004ab is similar to those of SN 2003du, SN 2005cf and SN 2011fe. The early-phase light curve of SN 2004ab in the *I* band looks similar to that of SN 2001el. After the secondary maximum, SN 2004ab is fainter than SN 2001el. The light curve of SN 2004ab is wider than that of SN 1996X in all the bands.

4 ANOMALOUS EXTINCTION OF THE HOST GALAXY TOWARDS SN 2004AB

SN 2004ab occurred very close to the nucleus of the host galaxy NGC 5054. Hence, a substantial amount of reddening caused by the interstellar medium (ISM) within the host galaxy is expected. The spectra of SN 2004ab show strong narrow Na I D absorption lines (see Section 6) in the rest frame of the host galaxy, with an average equivalent width (EW) of 3.3 Å. Matheson et al. (2004) also reported a similar EW of narrow Na I D lines. The measured EW gives a reddening of $E(B - V)_{\text{host}} = 0.53$ and 1.68 mag, on using the two relationships in Turatto, Benetti & Cappellaro (2003) between the EW of Na I D lines and $E(B - V)$.

The reddening suffered by SN 2004ab is also estimated using various photometric methods. The relationships between the observed SN colour at maximum and $\Delta m_{15}(B)$ (Phillips et al. 1999; Altavilla

Table 4. Photometric parameters of SN 2004ab.

Band	JD (max)[a]	m_λ^{max}	A_λ total	M_λ^{max}[b]	$\Delta m_{15}(\lambda)$	Decline rate[c] during 40–90 d
B	3056.8 ± 0.5	16.71 ± 0.05	4.15 ± 0.19	−19.31 ± 0.25	1.17 ± 0.05	-
V	3058.3 ± 0.5	15.11 ± 0.04	2.51 ± 0.11	−19.28 ± 0.19	0.64 ± 0.04	2.645
R	3059.6 ± 0.5	14.38 ± 0.05	1.82 ± 0.08	−19.31 ± 0.18	0.70 ± 0.05	3.352
I	3054.8 ± 0.5	13.90 ± 0.05	1.00 ± 0.04	−18.97 ± 0.16	0.66 ± 0.05	3.950

Notes. [a]245 0000+.
[b]For $\mu = 31.87$ and R_V(host) = 1.41.
[c]In unit of mag $(100\,\text{d})^{-1}$ and epoch is relative to the *B*-band maximum.
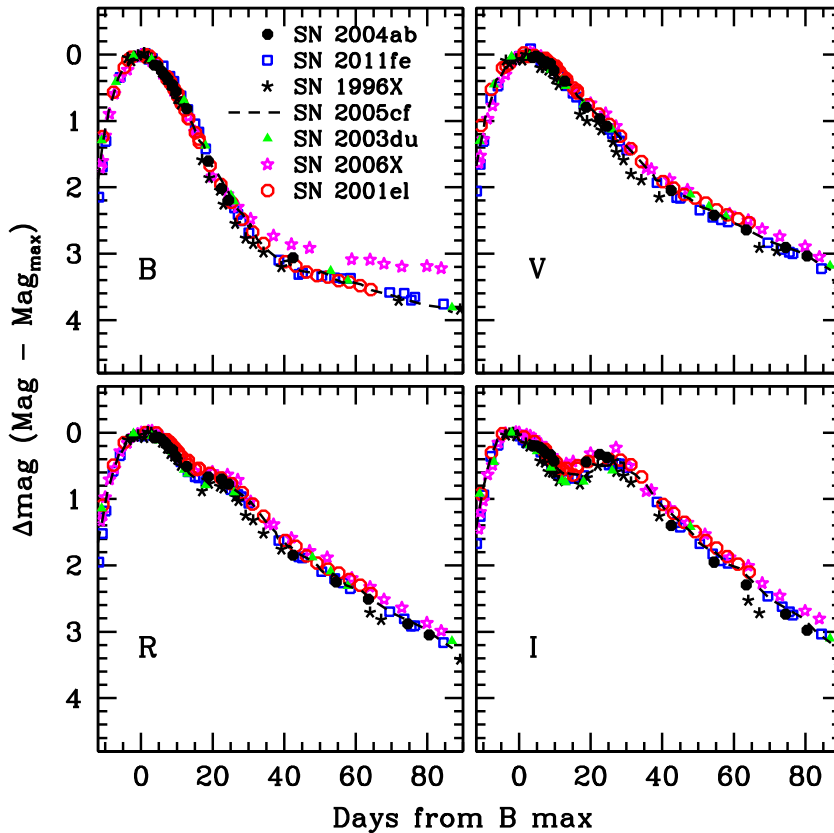
Figure 3. *BVRI* light curves of SN 2004ab compared with those of SN 1996X, SN 2001el, SN 2003du, SN 2005cf, SN 2006X and SN 2011fe. All the light curves have been shifted to match their peak magnitudes and to the epoch of the *B*-band maximum.

et al. 2004) give a total reddening of 1.65 mag. The relationship in Wang et al. (2006) between the $(B - V)$ colour measured at 12 d after the *B*-band maximum (referred as ΔC_{12}) and the decline-rate parameter gives $E(B - V)_{\text{total}}$ as 1.66 mag. The method of Reindl et al. (2005) gives a total reddening of 1.60 mag at maximum and 1.70 mag at 35 d after maximum. The average of all the reddening values derived using photometric methods is 1.65 ± 0.04 mag.

The contribution of reddening from the ISM within our Galaxy is $E(B - V)_{\text{Gal}} = 0.07$ (Schlegel, Finkbeiner & Davis 1998; Schlafly & Finkbeiner 2011). As an alternative method to estimating the reddening suffered by SN 2004ab, we compared the observed $(B - V)$ colour of SN 2004ab with the reddening-corrected $(B - V)$ colour curves of well-studied SNe Ia (see Fig. 4). The colour curves are dereddened using the reddening values given in the respective references. The $(B - V)$ colour curve of SN 2004ab was then shifted to match with the colour curves of the other SNe used in comparison. A χ^2 minimization was used to estimate the offset between the $(B - V)$ colour curve of SN 2004ab and those of other SNe. After shifting the $(B - V)$ colour curve of SN 2004ab by 1.70 ± 0.05 mag, it matches well with those of other SNe (see Fig. 4). This value of colour excess is consistent with the $E(B - V)_{\text{total}}$ derived using photometric and spectroscopic methods. For further analysis we use $E(B - V)_{\text{total}} = 1.70$ mag as the total reddening for SN 2004ab.

From the colour excess $E(B - V)$, the extinction in the *V* band, A_V, is estimated using the following relationship:

$$A_V = R_V \, E(B - V), \tag{1}$$

where R_V is the ratio of the total-to-selective extinction. Using the standard Galactic value of $R_V = 3.1$ and the estimated value of

$E(B - V) = 1.70$ mag, the above relationship gives a total extinction in the *V* band of $A_V = 5.27$ mag.

NGC 5054, the host galaxy of SN 2004ab, has a radial velocity corrected for Local Group infall onto the Virgo cluster of 1704 km s^{-1} (LEDA data base). Assuming $H_0 = 72$ km s^{-1} Mpc^{-1} (Freedman et al. 2001), we derived a distance modulus of $\mu = 31.87 \pm 0.15$ mag for NGC 5054. This leads to a *V*-band peak absolute magnitude of SN 2004ab of $M_V^{\text{max}} = -22.03 \pm 0.15$ mag, making it brighter by more than 2 mag than normal SNe Ia. This indicates that $R_V = 3.1$ is not applicable to the host galaxy component of extinction for SN 2004ab.

4.1 Estimation of R_V using photometry

Several studies have suggested lower values of R_V than its canonical value of 3.1 towards SNe Ia in their host galaxies (Elias-Rosa et al. 2006; Krisciunas et al. 2006, 2007; Wang et al. 2008; Folatelli et al. 2010; Amanullah et al. 2014). This indicates that the extinction properties of dust in the host galaxies towards SNe Ia is different from those in the Milky Way. The lower value of R_V is an indicator of smaller dust grains compared with those in the Milky Way. This type of dust is generally referred to as non-standard dust, and the reddening resulting from it as non-standard reddening. The extinction caused by dust in our Galaxy is explained with the model of Cardelli, Clayton & Mathis (1989), commonly known as the CCM model. Extinction in this model is parametrized by the following relationship:

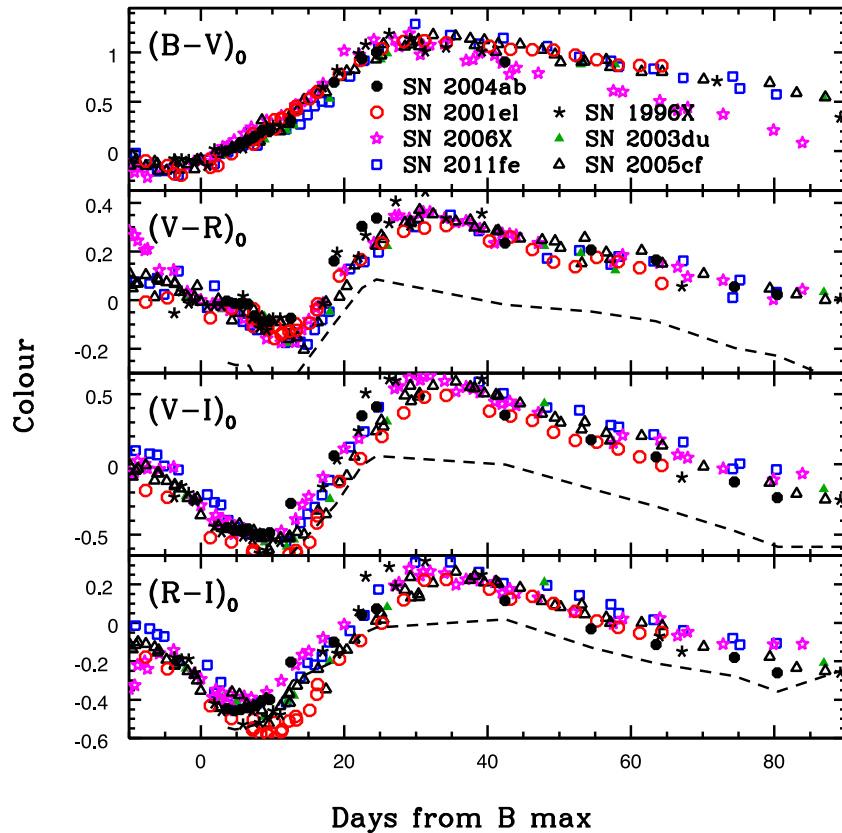$$\frac{A_\lambda}{A_V} = a_\lambda + \frac{b_\lambda}{R_V}, \tag{2}$$

Figure 4. The dereddened $(B - V)$, $(V - R)$, $(V - I)$ and $(R - I)$ colour curves of SN 2004ab plotted with those of some well-studied SNe Ia. The colour curves of SN 2004ab are corrected for $E(B - V)_{\rm Gal} = 0.07$ mag, $E(B - V)_{\rm host} = 1.63$ mag and $R_V({\rm host}) = 1.39$ using the CCM model with a_λ and b_λ coefficients from Krisciunas et al. (2006). The dashed lines represent dereddened colour curves of SN 2004ab if the coefficients from Cardelli, Clayton & Mathis (1989) are used.

where $A_V = R_V \, E(B - V)$, and a_λ and b_λ are wavelength-dependent coefficients. Krisciunas et al. (2006) have suggested that the coefficients of the reddening model for host galaxies of SNe Ia should be derived from the spectral energy distribution (SED) of SNe rather than from the SED of normal stars. They derived values of a_λ and b_λ for *UBVRI* bands using the Type Ia spectral template from Nugent, Kim & Perlmutter (2002). In order to estimate R_V towards SN 2004ab in the host galaxy, we used the dereddened colour curves of well-studied SNe Ia. The reddening-corrected $(B - V)$, $(V - R)$, $(V - I)$ and $(R - I)$ colour curves of these SNe are plotted in Fig. 4.

The colour curves of SN 2004ab were first corrected for the Galactic extinction of $E(B - V)_{\rm Gal} = 0.07$ mag, and then for $E(B - V)_{\rm host} = 1.63$ mag using the CCM extinction law with

varying R_V. A χ^2 minimization was used to estimate the value of R_V such that the dereddened $(V - R)$, $(V - I)$ and $(R - I)$ colour curves of SN 2004ab match with those of well-studied SNe Ia. It is found that with $R_V = 1.39 \pm 0.05$ and values of a_λ, b_λ as derived by Krisciunas et al. (2006), the dereddened colour curves of SN 2004ab match well with the colour curves of normal SNe Ia used in the comparison. Using this analysis we derived $E(V - R) = 0.64 \pm 0.06$ mag, $E(V - I) = 1.39 \pm 0.09$ mag and $E(R - I) = 0.75 \pm 0.07$ mag. The values of a_λ and b_λ from Cardelli et al. (1989) give a poor fit (shown by the dashed lines in Fig. 4). The derived value of $R_V = 1.39$ towards SN 2004ab in the host galaxy is smaller than the canonical value of $R_V = 3.1$ for the Milky Way. There are many host galaxies showing smaller value of R_V towards SNe Ia, some of which are listed in Table 5.

Table 5. The host galaxies with a low value of R_V towards SNe Ia.

| SN	Host galaxy	$\Delta m_{15}(B)_{\rm true}$	$E(B - V)_{\rm host}$	R_V	Reference
1999cl	NGC 4501	1.29 ± 0.08	1.24 ± 0.07	1.55 ± 0.08	Krisciunas et al. (2006)
2001el	NGC 1448	1.15 ± 0.04	0.21 ± 0.05	2.15 ± 0.23	Krisciunas et al. (2003)
2003cg	NGC 3169	1.25 ± 0.05	1.33 ± 0.11	1.80 ± 0.19	Elias-Rosa et al. (2006)
2005A	NGC 958	1.34 ± 0.03	1.11 ± 0.07	1.68 ± 0.10	Folatelli et al. (2010)
2006X	NGC 4321	1.31 ± 0.05	1.42 ± 0.04	1.48 ± 0.06	Wang et al. (2008)
2014J	M82	1.08 ± 0.03	1.37 ± 0.03	1.40 ± 0.10	Amanullah et al. (2014) Srivastav et al. (2016)
2004ab	NGC 5054	1.27 ± 0.05	1.63 ± 0.05	1.41 ± 0.06	This work
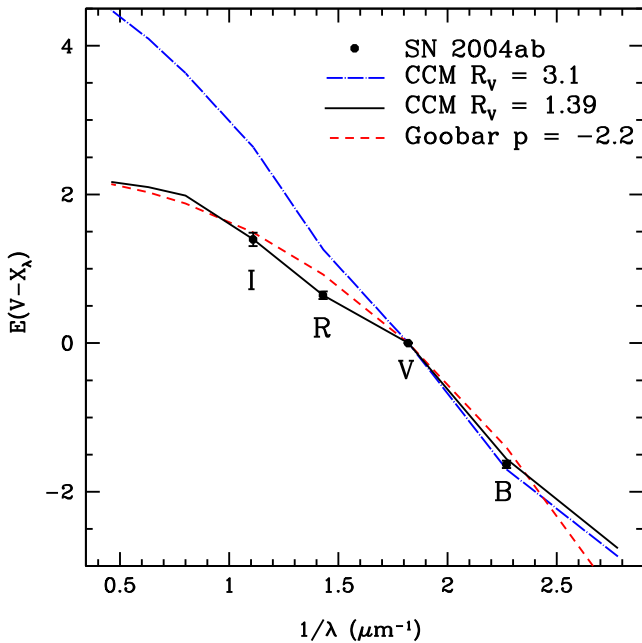
Figure 5. Colour excesses $E(V - X_\lambda)$, where $X_\lambda = BVRI$ measurement for SN 2004ab. The CCM extinction model $A_\lambda/A_V = a_\lambda + (b_\lambda/R_V)$ with $R_V = 3.1$, $R_V = 1.39$ and the power-law extinction model $A_\lambda/A_V = (\lambda/\lambda_V)^p$ of Goobar (2008) with $p = -2.2$ are also displayed.

As an alternative to CCM, the extinction model with a power law of type $A_\lambda/A_V = (\lambda/\lambda_V)^p$, expected from the multiple scattering of light owing to a dusty circumstellar material (CSM), is proposed (Goobar 2008; Amanullah et al. 2014). The multiple scattering of photons by circumstellar dust steepens the effective extinction law. The measured colour excess of SN 2004ab is fitted with this power law. A reasonably good fit is achieved for $p = -2.2$. The fit is shown in Fig. 5, along with the CCM model with $R_V = 1.39$ and $R_V = 3.1$.

4.2 Spectroscopic view of extinction

The anomalous extinction of SN 2004ab is also verified using the spectroscopic method described by Elias-Rosa et al. (2006). In this method, the optical SED of a reddened SN is compared with those of unreddened reference SNe Ia, at similar epochs. SN 1994D (Patat et al. 1996) and SN 1996X (Salvo et al. 2001), having similar decline-rate parameters, were selected as reference objects. All the spectra were dereddened for Galactic extinction and redshift-corrected. The reference spectra were then scaled to the distance of SN 2004ab. Extinction as a function of wavelength A_λ is derived using the formula

$$A_\lambda = -2.5 \log \frac{f_{04ab}}{f_{ref}^{scaled}}, \qquad (3)$$

where f_{04ab} and f_{ref}^{scaled} are the observed fluxes of SN 2004ab and the reference SN scaled to the distance of SN 2004ab, respectively. The extinction curve was obtained by normalizing the derived extinction A_λ at the V-band effective wavelength. We used three pairs of SN 1994D–2004ab and two pairs of SN 1996X–2004ab, a total five pairs of spectra for the analysis. In order to derive the value of R_V, we fitted the CCM model to extinction curves of SN 2004ab. Three examples of the fit are shown in Fig. 6. It is clear that the CCM model with $R_V = 3.1$ deviates for SN 2004ab, whereas the model extinction curve with the lower value of R_V ($\sim$1.4) fits the
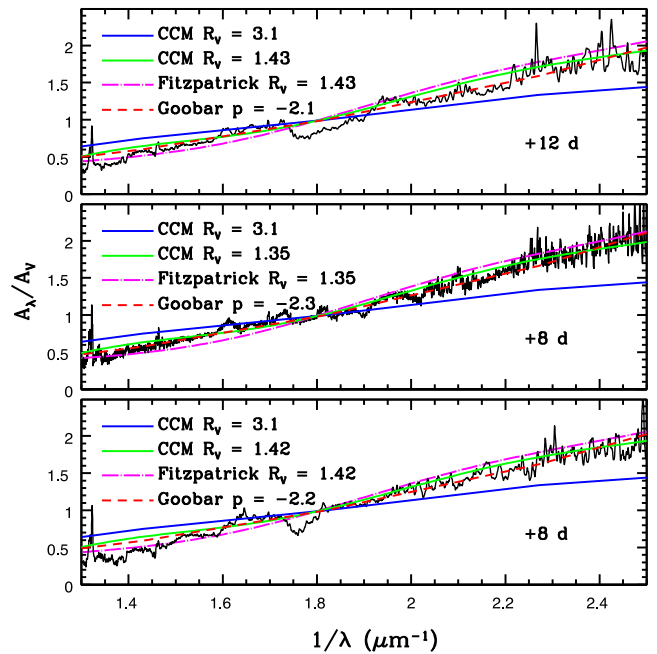

Figure 6. Extinction curve for SN 2004ab obtained using pairs of spectra of SN 1994D–2004ab (top and bottom panels) and SN 1996X–2004ab (middle panel). The best fits using the CCM extinction model $A_\lambda/A_V = a_\lambda + (b_\lambda/R_V)$, power-law extinction model $A_\lambda/A_V = (\lambda/\lambda_V)^p$ (Goobar 2008) and Fitzpatrick (1999) model are displayed. The standard Milky Way extinction law with $R_V = 3.1$ clearly deviates for SN 2004ab.

derived extinction curve reasonably well. The best-fitting values of R_V are also listed in Fig. 6. The derived extinction curve is also consistent with the Fitzpatrick parametrization (Fitzpatrick 1999) of an extinction curve with $R_V \sim 1.4$.

An attempt was made to fit the derived extinction curve of SN 2004ab with the power-law extinction model, $A_\lambda/A_V = (\lambda/\lambda_V)^p$, of Goobar (2008). The best-fitting model extinction curves and corresponding values of the power-law index p are shown in Fig. 6. From the analysis of five pairs of spectra we estimated a mean value of $R_V = 1.41 \pm 0.03$, which is similar to that derived from the photometric method. Combining the results obtained from the spectroscopic (five pairs of spectra) and photometric methods, we derived $R_V = 1.41 \pm 0.06$. This value of R_V is used in the analysis below.

5 ABSOLUTE AND BOLOMETRIC LUMINOSITY

The total extinctions A_λ suffered by SN 2004ab in the $BVRI$ bands were derived (using $R_V^{host} = 1.41$) as 4.15 ± 0.19, 2.51 ± 0.11, 1.82 ± 0.08 and 1.00 ± 0.04 mag, respectively. Using these values and a distance modulus of $\mu = 31.87$ mag, the peak absolute magnitudes in different bands were calculated and are listed in Table 4.

Alternatively, the peak absolute magnitudes can also be estimated using the empirical *luminosity decline-rate relationship*. Peak absolute magnitudes of type Ia SNe are known to be correlated with $\Delta m_{15}(B)$ (Phillips et al. 1999). Using the calibration in Folatelli et al. (2010), we derived the B-band peak absolute magnitude of SN 2004ab as -19.24 ± 0.20 mag, consistent with the value given in Table 4.
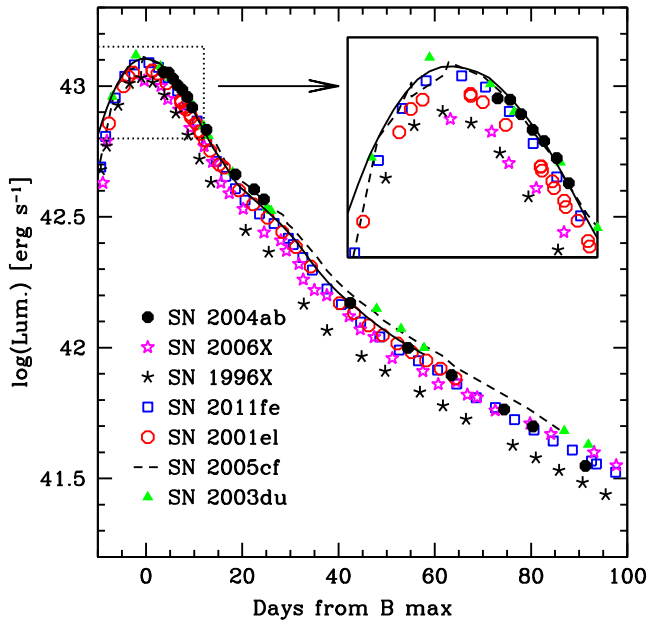
Figure 7. The quasi-bolometric light curve of SN 2004ab is plotted along with those of other well-studied SNe Ia. The solid line represents the quasi-bolometric light curve derived using the SNOOPY fit to the observed data points. A zoomed view of the plot around the peak is shown in the inset.

The bolometric flux of SN 2004ab was obtained using the observed *BVRI* magnitudes listed in Table 2. The magnitudes were corrected for total extinction. The extinction-corrected magnitudes were converted to flux using the zero-points from Bessell, Castelli & Plez (1998). A distance modulus of $\mu = 31.87 \pm 0.15$ mag was used to estimate the bolometric luminosity. Because SN 2004ab was observed in the *BVRI* bands, in order to account for the missing fluxes we applied a correction as described by Wang et al. (2009b). The quasi-bolometric light curve of SN 2004ab is plotted in Fig. 7 and compared with those of other SNe Ia. The bolometric light curve of SN 2004ab is similar to those of SN 2001el and SN 2011fe. The peak bolometric luminosity of SN 2004ab was estimated as $\log L_{\rm bol}^{\max} = 43.10 \pm 0.07$ erg s^{-1}.

5.1 Mass of nickel synthesized

The mass of ^{56}Ni synthesized in the explosion of SN 2004ab was estimated using Arnett's rule (Arnett 1982). SN 2004ab was discovered on 2004 February 21.98. It was not detected on 2004 February 1.15 up to a limiting magnitude of 18 mag (Monard & Vanmunster 2004). The bolometric light curve peaked on 2004 February 21.32. This indicates that the rise time $t_{\rm R} < 20$ d for SN 2004ab. The rise time of SNe Ia is found to be correlated with $\Delta m_{15}(B)$. Brighter SNe with a smaller $\Delta m_{15}(B)$ have a longer rise time, and fainter SNe with a larger $\Delta m_{15}(B)$ have a shorter rise time. The spectroscopically normal SNe Ia have a typical rise time of 18–19.5 d (Riess et al. 1999; Conley et al. 2006; Ganeshalingam, Li & Filippenko 2011). The post-maximum decline-rate and rise-time relationship in Pskovskii (1984) gives $t_{\rm R} = 19$ d for SN 2004ab. Using $t_{\rm R} = 19$ d, a peak bolometric luminosity of $\log L_{\rm bol}^{\max} = 43.10$ erg s^{-1} and $\alpha = 1.2$ (Branch 1992), the mass of ^{56}Ni synthesized in the explosion of SN 2004ab was estimated to be $M_{\rm Ni} = 0.53 \pm 0.08$ M$_\odot$.
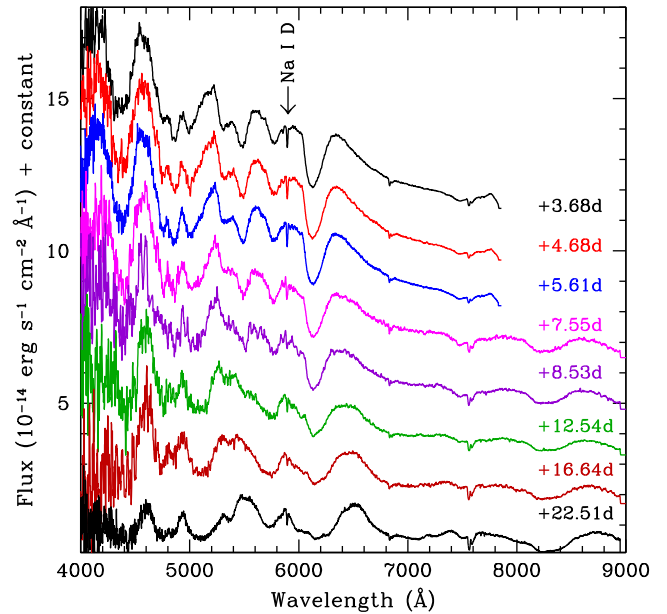

Figure 8. Spectral evolution of SN 2004ab from +3.7 to +22.5 d. The strong narrow Na I D feature from the host galaxy is clearly seen.
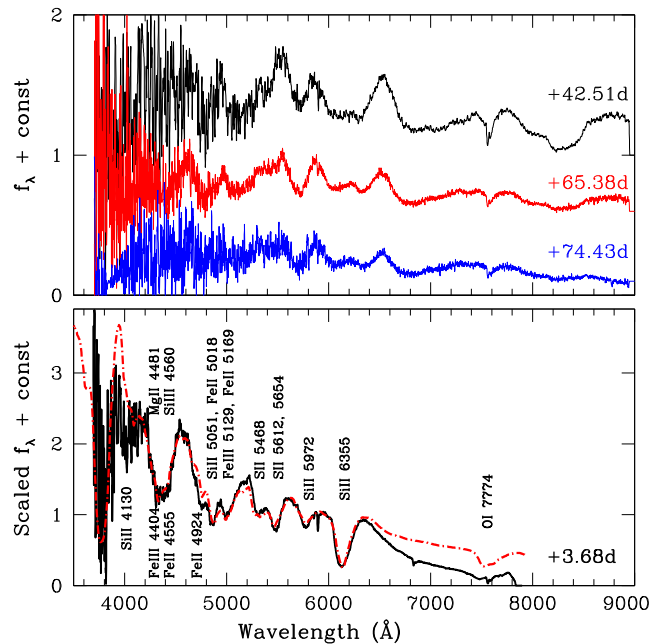

Figure 9. Top: Spectral evolution of SN 2004ab from +42.5 to +74.4 d. Bottom: The synthetic spectrum generated using the SYN++ code is compared with that of SN 2004ab at +3.7 d.

6 SPECTROSCOPIC RESULTS

6.1 Spectral evolution

We obtained 11 spectra of SN 2004ab spanning from +3.7 to +74.4 d with respect to the *B*-band maximum. The details of the observations are given in Table 3. The spectral evolution of SN 2004ab from +3.7 to +22.5 d is presented in Fig. 8, and from +42.5 to +74.4 d in Fig. 9. All the spectra have been corrected
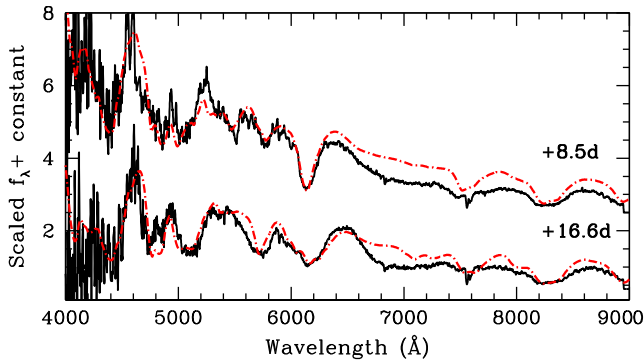
Figure 10. The synthetic spectra generated using the SYN++ code are compared with those of SN 2004ab at +8.5 and +16.6 d.

for reddening (using $R_V^{host} = 1.41$), as discussed in Section 4, and redshift $z = 0.0058$.

The first spectrum of SN 2004ab, obtained on +3.7 d, shows the features seen in normal SNe Ia. The Fe III $\lambda 4404$, Mg II $\lambda 4481$, Fe II $\lambda 4555$ and Si III $\lambda 4560$ lines are blended, giving a broad and deep profile in the region 4200–4600 Å. During subsequent evolution, lines due to Fe III, Si III weaken, and the profile narrows. Features of Fe II $\lambda\lambda 4924$, 5018, Si II λ 5051, Fe III $\lambda 5129$ and Fe II $\lambda 5169$ are clearly visible in the 4600–5200 Å spectral region. The 'W'-shaped S II $\lambda\lambda 5654$, 5468, Si II $\lambda 5972$ and Si II $\lambda 6355$ characteristics of normal SNe Ia are strong in the spectrum of SN 2004ab. The strong narrow feature seen between Si II $\lambda 5972$ and Si II $\lambda 6355$ is a result of Na I D from the host galaxy, indicating the high reddening within the SN host. The overall appearances of the first three spectra, corresponding to +3.7, +4.7 and +5.6 d, are identical. The spectrum obtained on +7.6 d also covers the red region, where O I and the Ca II near-infrared (NIR) triplet are clearly seen. The 'W'-shaped S II lines are weaker. By +12.5 d, most of the Fe II lines are stronger, and the S II feature is hardly visible. In the spectrum at +22.5 d, the Fe II lines are well developed, and the Si II $\lambda 6355$ is being replaced by a broad absorption profile owing to the increased contamination of Fe II lines.

The spectrum at +42.5 d, shown in Fig. 9, is dominated by strong Fe II $\lambda 4924$, $\lambda 5018$, $\lambda 5169$, $\lambda 5536$, Na I, and the Ca II NIR triplet. The spectral appearance of the next two spectra obtained at +65.4 and +74.4 d is similar, except for the weakening of the Ca II NIR triplet.

The spectrum of SN 2004ab at +3.7 d was fitted with a synthetic spectrum generated using the SYN++ code (Thomas, Nugent & Meza 2011) and shown in Fig. 9. The best fit to the observed spectrum was achieved at a photospheric velocity of 10 700 km s^{-1} and a blackbody temperature of 14 000 K. In order to reproduce the observed features, ions of O I, Na I, Mg II, Si II, Si III, S II, Ca II, Fe II and Fe III, each at an excitation temperature of 7000 K, were included in the synthetic spectrum. The optical depth of each absorption feature was set to decrease exponentially with velocity, keeping the *e*-folding velocity at 1000 km s^{-1}. The identified features are marked on the spectrum.

The synthetic spectra at +8.5 and +16.6 d were also generated and are displayed in Fig. 10, along with the observed spectra. The best fit for the spectrum at +8.5 d was obtained using a photospheric velocity of 10 500 km s^{-1} and a blackbody temperature of 13a,000 K. The ions included to reproduce the synthetic spectrum are the same as those for +3.7 d. For the spectrum at +16.6 d, the photospheric velocity is set to 9500 km s^{-1} and the blackbody
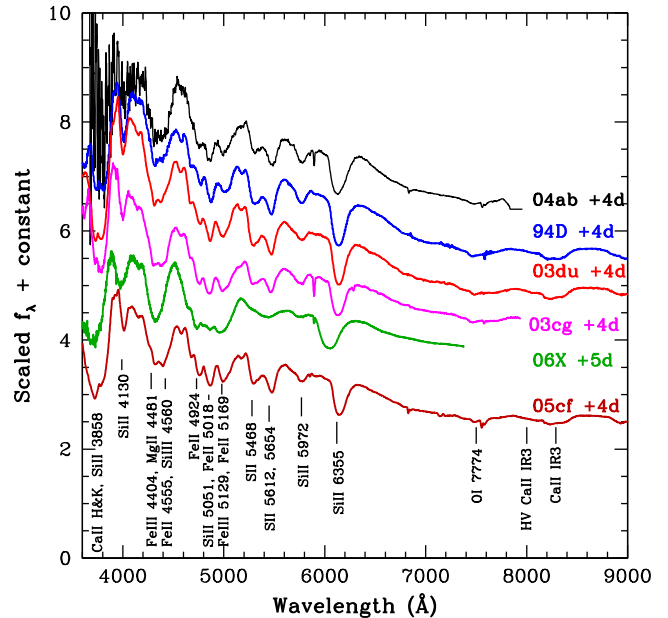

Figure 11. Comparison of spectra of SN 2004ab and those of other well-studied SNe Ia at +4 d.
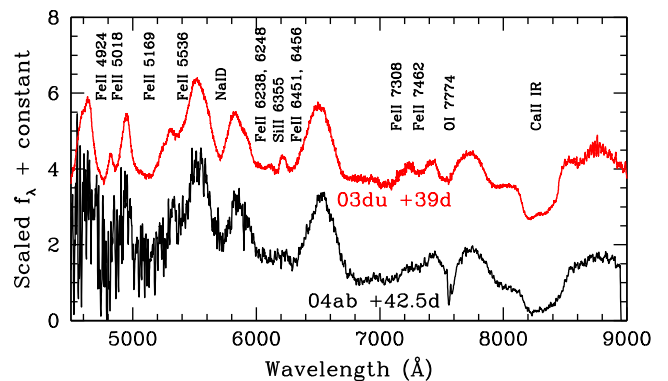

Figure 12. Comparison of the spectra of SN 2004ab and SN 2003du at +42.5 d.

temperature to 10 000 K. The synthetic spectrum includes ions of O I, Na I, Mg II, Si II, Ca II and Fe II.

In Fig. 11, the spectrum of SN 2004ab at ∼+4 d is compared with those of SN 1994D (Patat et al. 1996), SN 2003du (Anupama et al. 2005), SN 2003cg (Elias-Rosa et al. 2006), SN 2006X (Wang et al. 2008) and SN 2005cf (Garavini et al. 2007; Wang et al. 2009b) at similar epochs. The comparison spectra were obtained from SUSPECT[2] and WISeREP[3] Supernova Spectrum Archives.

The spectrum of SN 2004ab is similar to those of other SNe. Although SN 2006X was a highly reddened SN similar to SN 2004ab, it had a greater expansion velocity and hence most of the features are blended. The extreme blue region of the SN 2004ab spectrum is quite noisy. However, the Ca II H&K, Si II $\lambda 3858$ and Si II $\lambda 4130$ features are clearly visible.

The spectrum of SN 2004ab at +42.5 d is compared with that of SN 2003du in Fig. 12. It is clear that the spectrum of SN 2004ab is very similar to that of SN 2003du. The spectra of both SNe are
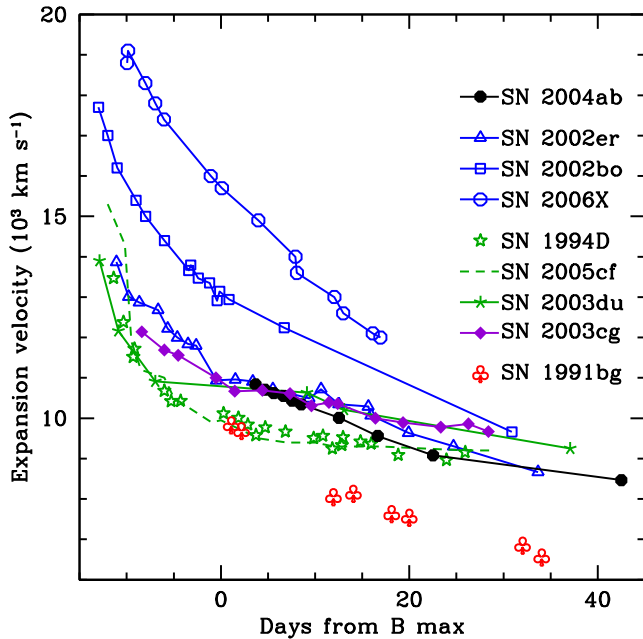
---

[2] http://www.nhn.ou.edu/ suspect/

[3] http://www.weizmann.ac.il/astrophysics/wiserep/

Figure 13. The velocity evolution of the Si II λ6355 absorption line for SN 2004ab is compared with those of other SNe Ia.

Figure 14. Spectroscopic subclassification of SN 2004ab based on the scheme of Benetti et al. (2005). Transitional events from Pastorello et al. (2007a) and Sahu et al. (2013) are included.

characterized by strong Fe II lines. Other features such as Na I and the Ca II NIR triplet are very strong and similar in the spectra of SN 2004ab and SN 2003du. The overall spectral evolution of SN 2004ab is very similar to that of normal SNe Ia.

6.2 Expansion velocity

The photospheric velocity measured from the Si II λ6355 absorption line in the spectra of SN 2004ab is plotted in Fig. 13 and compared with those of other SNe Ia. SN 2004ab was discovered late, and hence there is no early phase-velocity information for this supernova. At +3.7 d, SN 2004ab has a photospheric velocity of $\sim 10\,800\,\mathrm{km\,s^{-1}}$, similar to those of SN 2002er, SN 2003cg and SN 2003du, but higher than those of SN 1994D and SN 2005cf, and lower than the high-velocity SNe Ia SN 2002bo and SN 2006X. One week after the *B*-band maximum, the velocity of SN 2004ab decreases to $\sim 10\,500\,\mathrm{km\,s^{-1}}$, and after two weeks it is $\sim 9000\,\mathrm{km\,s^{-1}}$. At the last data point, which corresponds to +42.5 d, the velocity of the Si II λ6355 absorption line is $\sim 8500\,\mathrm{km\,s^{-1}}$.

The expansion velocity of normal SNe Ia shows a rapid temporal evolution during the pre-maximum phase, and after the *B*-band maximum the expansion velocity changes slowly. From Fig. 13, it is clear that SN 2004ab follows a trend similar to that of SN 2002er. The velocity evolutions of the two SNe are very similar.

6.3 Spectroscopic parameter

Based on the gradient of the velocity evolution of the Si II λ6355 line, Benetti et al. (2005) grouped SNe Ia into three subclasses. The SNe showing very slow velocity evolution and hence low velocity gradients in the post-maximum phase are termed Low Velocity Gradient (LVG; velocity gradient $\dot{v} < 60$–$70\,\mathrm{km\,s^{-1}\,d^{-1}}$) events. SN 1994D, SN 2003du and SN 2005cf fall into this subgroup. On the other hand, SNe such as SN 2002er, SN 2002bo and SN 2006X having high velocity gradients are called High Velocity Gradient
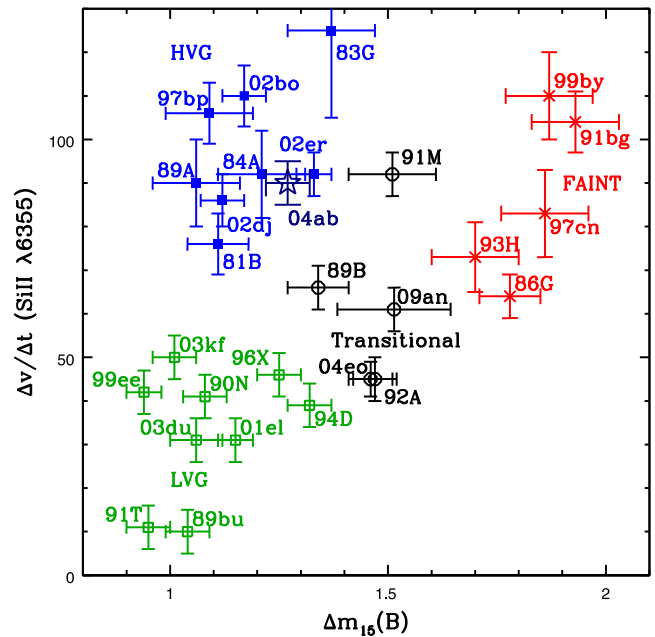
(HVG) events. The LVG group includes luminous and normal SNe Ia, while the HVG group has average luminosity. Under-luminous SNe such as SN 1991bg show a high velocity gradient, and are grouped under the Faint subclass. The measured velocity gradient of SN 2004ab is $90\,\mathrm{km\,s^{-1}\,d^{-1}}$, which falls in the HVG subclass. The classification scheme of Benetti et al. (2005) is shown in Fig. 14, and the position of SN 2004ab is marked on it. SN 2004ab is near SN 2002er in the clustered region of HVG events. The average luminosity of SN 2004ab is consistent with its belonging to the HVG group.

Branch et al. (2006) introduced another method of classifying SNe Ia spectroscopically, using the pseudo-EWs of the Si II λ5972 (W(5750)) and Si II λ6355 (W(6100)) lines in the spectrum around the *B*-band maximum. In a plot of W(5750) against W(6100), the SNe are distributed in four regions of shallow silicon (SS; SN 1991T-like), core normal (CN; SN 2003du-like), broad line (BL; SN 2002bo-like) and cool (CL; SN 1991bg-like). The classification scheme of Branch et al. (2006) is shown in Fig. 15, with the position of SN 2004ab marked. It falls in the region occupied by BL objects. The HVG objects have properties overlapping with those of the BL group. This also holds for SN 2004ab.

The strength ratio of the Si II λ5972 and Si II λ6355 lines is correlated with the luminosity of SNe Ia (Nugent et al. 1995; Benetti et al. 2005). The value of $\mathcal{R}(\mathrm{Si\,II})$ is found to be smaller for luminous objects and larger for, fainter objects. We measured the line strength ratio, $\mathcal{R}(\mathrm{Si\,II})$, for SN 2004ab as 0.37 and plotted it against $\Delta m_{15}(B)$ in Fig. 16, along with other SNe Ia from Benetti et al. (2005), Pastorello et al. (2007a) and Sahu, Anupama & Anto (2013). SN 2004ab is situated near SN 1994D within the diagonal strip of Fig. 16.

Using the expansion velocity estimated from the Si II line in the spectrum close to maximum light, Wang et al. (2009a) grouped SNe Ia into two classes: those having high velocity (HV), $v \geq 11\,800\,\mathrm{km\,s^{-1}}$, and others having normal velocity (NV), with an average of $\langle v \rangle = 10\,600\,\mathrm{km\,s^{-1}}$. Because SN 2004ab was discovered
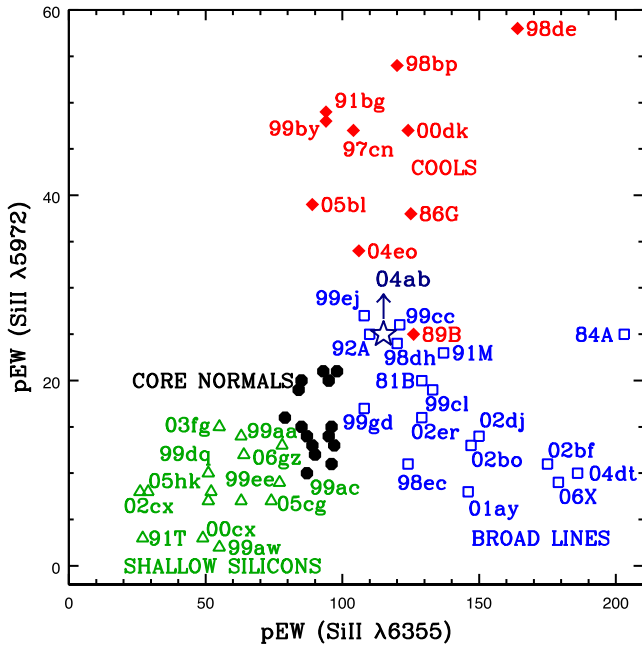
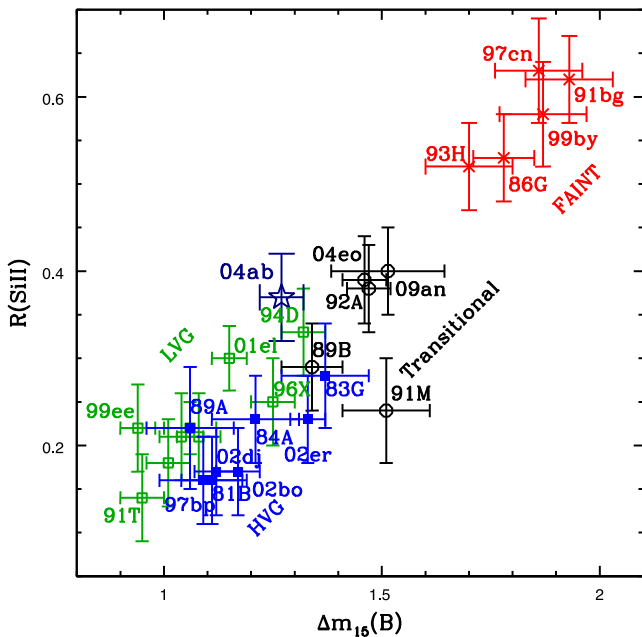**Figure 15.** Spectroscopic subclassification of SN 2004ab based on the scheme of Branch et al. (2006).

Figure 16. $\mathcal{R}(\text{Si}\,\textsc{ii})$ ratio versus $\Delta m_{15}(B)$ plot for SN 2004ab and other SNe Ia from Benetti et al. (2005), Pastorello et al. (2007a) and Sahu et al. (2013).

late, our first spectrum was obtained 3.7 d after maximum light. Hence, the exact value of the velocity at maximum light could not be determined. However, from the observed trend in velocity evolution (see Fig. 13), it is inferred that at maximum light it would have a velocity of ∼11 000 km s⁻¹, and hence can be considered as a NV type. Wang et al. (2009a) found that R_V was lower (∼1.6) for the HV than for the NV (∼2.4) subgroup in their sample. However, Foley & Kasen (2011) found that, after excluding highly reddened SNe having ($E(B - V) > 0.35$) from the sample of Wang et al. (2009a), both the NV and the HV subgroup are consistent with the

same value of $R_V = 2.5$. SN 2004ab seems to be a NV SN and has a very low value of $R_V = 1.41$.

The velocity evolution and gradient of SN 2004ab match well with those of SN 2002er (see Figs 13 and 14). Both SNe show high gradients in their velocities. However, there is no similarity in the line strength ratio, $\mathcal{R}(\text{Si}\,\textsc{ii})$, of these two SNe. The $\mathcal{R}(\text{Si}\,\textsc{ii})$ of SN 2004ab is higher than that of SN 2002er. The $\mathcal{R}(\text{Si}\,\textsc{ii})$ value of SN 2004ab is more like that of LVG SNe, while SN 2002er follows other HVG SNe. This is because the Si\,\textsc{ii} λ5972 line is stronger in SN 2004ab that in SN 2002er. Many HVG SNe overlap with the BL type, and this is also true for SN 2004ab. But unlike most other BLs, which have strong Si\,\textsc{ii} λ6355 line and relatively weaker Si\,\textsc{ii} λ5972, SN 2004ab has a stronger Si\,\textsc{ii} λ5972 line and a weaker Si\,\textsc{ii} λ6355 line.

7 SUMMARY

We have presented optical photometric and spectroscopic analyses of SN 2004ab. SN 2004ab is a highly reddened normal Type Ia supernova with $E(B - V)_{\text{total}} = 1.70$ mag. The intrinsic decline-rate parameter of SN 2004ab is $\Delta m_{15}(B)_{\text{true}} = 1.27$. The photospheric velocity evolution measured from the Si\,\textsc{ii} λ6355 absorption line is similar to that of SN 2002er. The Si\,\textsc{ii} λ6355 velocity gradient is estimated as $\dot{v} = 90$ km s⁻¹ d⁻¹, indicating that SN 2004ab is a member of the HVG subgroup. The pseudo-EWs of the Si\,\textsc{ii} λ5972 and λ6355 absorption lines suggest that SN 2004ab is a BL type. The line strength ratio $\mathcal{R}(\text{Si}\,\textsc{ii})$ is 0.37, higher than those of other BLs having similar $\Delta m_{15}(B)$. This is a result of the higher strength of Si\,\textsc{ii} λ5972 in SN 2004ab. Using the CCM model, the ratio of the total-to-selective extinction for the host galaxy NGC 5054, in the direction of SN 2004ab, is derived as $R_V = 1.41$, which is much lower than that for the Milky Way. The derived extinction is also consistent with a power-law extinction model $A_\lambda / A_V = (\lambda / \lambda_V)^p$ with $p \sim -2.2$. SN 2004ab peaked at an absolute magnitude of $M_B^{\text{max}} = -19.31 \pm 0.25$ mag. The peak bolometric luminosity of log $L_{\text{bol}}^{\text{max}} = 43.10 \pm 0.07$ erg s⁻¹ suggests that 0.53 ± 0.08 M$_\odot$ of ^{56}Ni was synthesized in this explosion. Although SN 2004ab is a highly reddened supernova, its absolute luminosity, after correcting for extinction using the non-standard extinction law, is similar to that of a normal SN Ia and follows the empirical *luminosity decline-rate relationship*.

Dodge Department of Physics and Astronomy, University of Oklahoma and WISeREP maintained by the Weizmann Institute of Science computing centre.

REFERENCES

Altavilla G. et al., 2004, MNRAS, 349, 1344
Amanullah R. et al., 2014, ApJ, 788, L21
Anupama G. C., Sahu D. K., Jose J., 2005, A&A, 429, 667
Arnett W. D., 1982, ApJ, 253, 785
Benetti S. et al., 2005, ApJ, 623, 1011
Bessell M. S., Castelli F., Plez B., 1998, A&A, 337, 321
Branch D., 1992, ApJ, 392, 35
Branch D. et al., 2006, PASP, 118, 560
Burns C. R. et al., 2011, AJ, 141, 19
Cardelli J. A., Clayton G. C., Mathis J. S., 1989, ApJ, 345, 245
Chandrasekhar S., 1931, ApJ, 74, 81
Chotard N. et al., 2011, A&A, 529, L4
Conley A. et al., 2006, AJ, 132, 1707
Elias-Rosa N. et al., 2006, MNRAS, 369, 1880
Fitzpatrick E. L., 1999, PASP, 111, 63
Folatelli G. et al., 2010, AJ, 139, 120
Foley R. J., Kasen D., 2011, ApJ, 729, 55
Freedman W. L. et al., 2001, ApJ, 553, 47
Ganeshalingam M., Li W., Filippenko A. V., 2011, MNRAS, 416, 2607
Garavini G. et al., 2007, A&A, 471, 527
Goobar A., 2008, ApJ, 686, L103
Howell D. A., 2011, Nature Comm., 2, 350
Hoyle F., Fowler W. A., 1960, ApJ, 132, 565
Iben I., Jr, Tutukov A. V., 1984, ApJS, 54, 335
Jha S., Riess A. G., Kirshner R. P., 2007, ApJ, 659, 122
Krisciunas K. et al., 2003, AJ, 125, 166
Krisciunas K., Prieto J. L., Garnavich P. M., Riley J. L. G., Rest A., Stubbs C., McMillan R., 2006, AJ, 131, 1639
Krisciunas K. et al., 2007, AJ, 133, 58
Landolt A. U., 1992, AJ, 104, 340
Mandel K. S., Narayan G., Kirshner R. P., 2011, ApJ, 731, 120
Maoz D., Mannucci F., Nelemans G., 2014, ARA&A, 52, 107
Matheson T., Challis P., Kirshner R., Berlind P., Huchra J., 2004, IAU Circ., 8293, 2
Monard L. A. G., Vanmunster T., 2004, Cent. Bur. Elect. Teleg., 61, 1
Nugent P., Phillips M., Baron E., Branch D., Hauschildt P., 1995, ApJ, 455, L147
Nugent P., Kim A., Perlmutter S., 2002, PASP, 114, 803
Pastorello A. et al., 2007a, MNRAS, 377, 1531
Pastorello A. et al., 2007b, MNRAS, 376, 1301
Patat F., Benetti S., Cappellaro E., Danziger I. J., della Valle M., Mazzali P. A., Turatto M., 1996, MNRAS, 278, 111
Perlmutter S. et al., 1997, ApJ, 483, 565
Phillips M. M., 1993, ApJ, 413, L105
Phillips M. M., 2012, PASA, 29, 434
Phillips M. M., Lira P., Suntzeff N. B., Schommer R. A., Hamuy M., Maza J., 1999, AJ, 118, 1766
Pisano D. J., Barnes D. G., Staveley-Smith L., Gibson B. K., Kilborn V. A., Freeman K. C., 2011, ApJS, 197, 28
Pskovskii Y. P., 1984, Soviet Ast., 28, 658
Reindl B., Tammann G. A., Sandage A., Saha A., 2005, ApJ, 624, 532
Richmond M. W., Smith H. A., 2012, J. Am. Assoc. Variable Star Obs., 40, 872
Riess A. G., Press W. H., Kirshner R. P., 1996, ApJ, 473, 88
Riess A. G. et al., 1999, AJ, 118, 2675
Sahu D. K., Anupama G. C., Anto P., 2013, MNRAS, 430, 869
Salvo M. E., Cappellaro E., Mazzali P. A., Benetti S., Danziger I. J., Patat F., Turatto M., 2001, MNRAS, 321, 254
Schlafly E. F., Finkbeiner D. P., 2011, ApJ, 737, 103
Schlegel D. J., Finkbeiner D. P., Davis M., 1998, ApJ, 500, 525
Scolnic D. M., Riess A. G., Foley R. J., Rest A., Rodney S. A., Brout D. J., Jones D. O., 2014, ApJ, 780, 37
Srivastav S., Ninan J. P., Kumar B., Anupama G. C., Sahu D. K., Ojha D. K., Prabhu T. P., 2016, MNRAS, 457, 1000
Stanishev V. et al., 2007, A&A, 469, 645
Thomas R. C., Nugent P. E., Meza J. C., 2011, PASP, 123, 237
Turatto M., Benetti S., Cappellaro E., 2003, in Hillebrandt W., Leibundgut B., eds, Proc. ESO/MPA/MPE Workshop, From Twilight to Highlight: The Physics of Supernovae. Springer, Berlin, p. 200
Vinkó J. et al., 2012, A&A, 546, A12
Wang L., 2005, ApJ, 635, L33
Wang X., Wang L., Pain R., Zhou X., Li Z., 2006, ApJ, 645, 488
Wang X. et al., 2008, ApJ, 675, 626
Wang X. et al., 2009a, ApJ, 699, L139
Wang X. et al., 2009b, ApJ, 697, 380
Webbink R. F., 1984, ApJ, 277, 355
Whelan J., Iben I., Jr, 1973, ApJ, 186, 1007

This paper has been typeset from a TEX/LATEX file prepared by the author.